99-06

NATIONAL WATER RESEARCH INSTITUTE

INSTITUT NATIONAL DE RECHERCHE SUR LES EAUX

^{210}Pb Dating of Sediments from the St. Lawrence River (Station 179 Core 214), Ontario

L.J. Turner

Report No. 99-06

April 1999

AECB/NWRI

^{210}Pb Dating of Sediments from the St. Lawrence River (Station 179, Core 214), Ontario.

L.J. Turner

Report 99-6
April 1999

National Water Research Institute
Canada Centre for Inland Waters
Burlington, Ontario L7R 4A6

Turner, L.J., 1999. ^{210}Pb Dating of Sediments from the St. Lawrence River (Station 179,Core 214), Ontario. National Water Research Institute, Burlington, Ontario. NWRI Report 99-6, 25p.

SUMMARY

A sediment core was dated from the St. Lawrence River near Cornwall, Ontario. The ^{210}Pb activity profile of the sediment core was used to determine the chronological age of the sediment as well as the sedimentation rate. The mean specific gravity was determined to be 2.589 $g \cdot cm^{-3}$. Data were analysed using two types of models: the Constant Initial Concentration (CIC) model and the Constant Rate of Supply (CRS) model. Deposition rates and chronology determined from the CIC models were in excellent agreement. Deposition rate determined from the CRS model agreed well with CIC model results. CRS chronology was within error of the CIC model chronologies.

The sedimentation rate was calculated to be 1.05 $cm \cdot yr^{-1}$ for core 214 using the CIC1 model. The average mass sedimentation rate was determined to be 0.26 $g \cdot cm^{-2} \cdot yr^{-1}$ using the CIC1 model, 0.25 $g \cdot cm^{-2} \cdot yr^{-1}$ using the CIC2 model, and 0.26 ± 0.06 $g \cdot cm^{-2} \cdot yr^{-1}$ using the CRS model. Porosity analysis indicates a slight change in sediment composition which may be accompanied by varying accumulation rate. CRS results also indicate a slight variability in sedimentation rate in this core. Sediment focusing factors calculated from CIC and CRS outputs range from 2.6 to 2.4.

INTRODUCTION

In this study, a core (214) taken from Station 179 in the St. Lawrence River, was dated using a ^{210}Pb method (Eakins and Morrison, 1978). The core was collected and submitted by Norm Rukavina (NWRI). Other cores from this area have been analyzed using this method (Turner 1999a-b, 1996 a-g).

LOCATION AND CORE PREPARATION

The location of the sample site (Station 179) from which the core was taken (UTM Coordinates: 4984798.6 N, 525940 E) is shown in Figure 1. The site is near Cornwall, Ontario. On November 19, 1997, the St. Lawrence River was cored by divers using benthos coring tubes (6.6 cm inner diameter). Several cores were collected from the site. The cores were transported to NWRI in Burlington and placed in cold storage. On February 2, 1999, one of the cores (179-1) was split in half lengthwise. One of the halves was then subsectioned into 1-cm intervals giving forty-one (41) samples. The samples were weighed, freeze-dried, and then re-weighed. These weights were used to calculate porosity and the uncompacted depth (see Appendices A - B, Delorme, 1991).

A plot of porosity versus cumulative dry weight for core 214 is shown in Figure 2a. This figure indicates the composition of the sediments to be slightly variable. A small zone of elevated porosity exists just below the top of the core. A decrease in porosity occurs near the bottom of the core.

Specific Gravity was determined using an automated Accupyc pycnometer (Micromeritics, 1992). Figure 2b is a plot of specific gravity (or density) versus cumulative dry weight. Figure 2b indicates a fairly stable sediment composition with only a slight increase in density with depth. Mean specific gravity for the sediments of core 214 is 2.589 ± 0.037 $g cm^{-3}$ based on 5 samples and 25 determinations (see Appendix C this report).

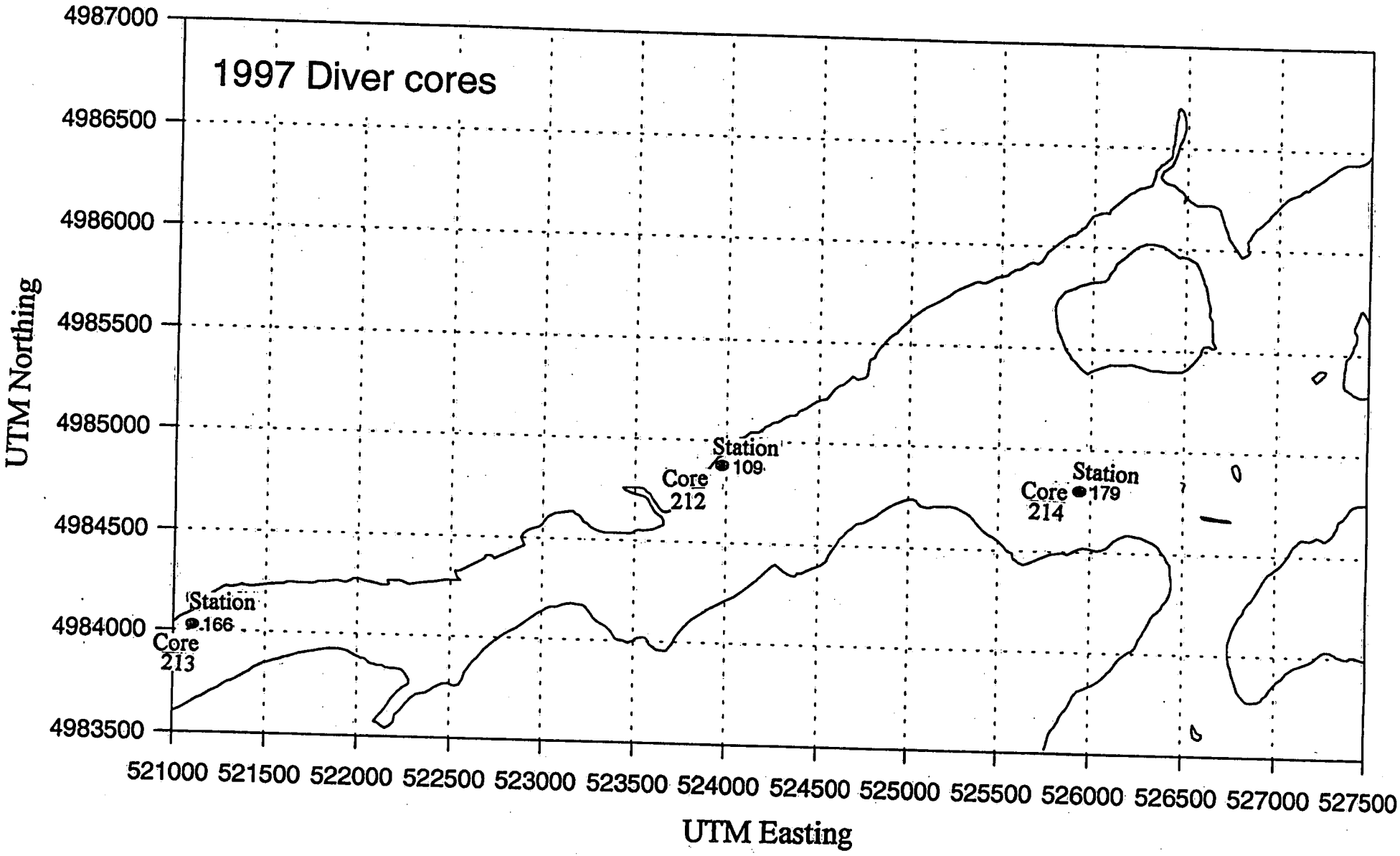

Figure 1. Location map of the sampling site for core 214.

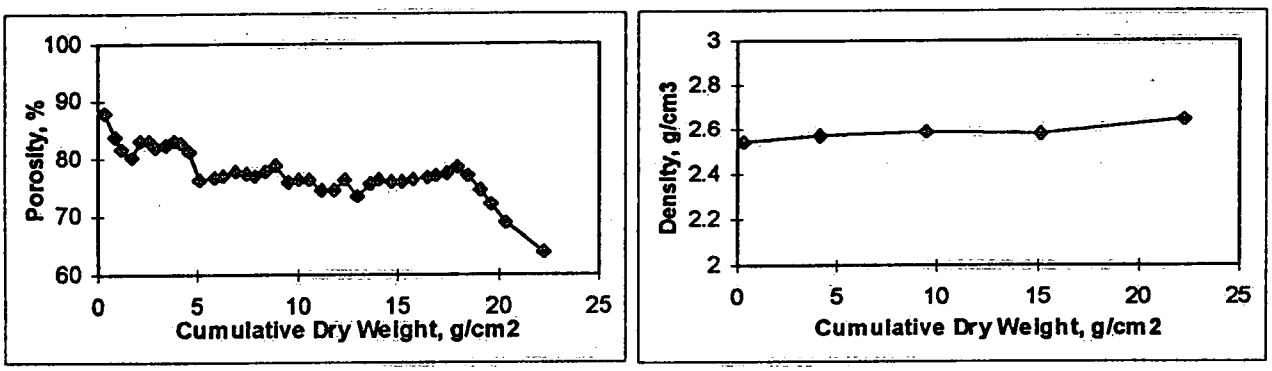

Figure 2. Relationship between cumulative dry weight and (a) porosity, (b) density.

METHOD

Laboratory Procedures

Homogeneous portions of 19 samples (Table 1, including 1 set of replicates) from core 214 were treated using a variation on the Eakins and Morrison (1978) polonium distillation procedure. Details of the laboratory procedure are found in a laboratory manual (Turner, 1990).

Following grinding and homogenizing, 1 g of sediment was treated with concentrated HCl to remove carbonate materials, then mixed with approximately 10 dpm of ^{209}Po spike in a test tube. The ^{209}Po spike was prepared on September 6, 1991 at 6.07 dpm ml^{-1} activity. The test tube and contents were then placed in an oven at 110°C until dry.

After cooling, glass wool plugs (one to hold the sediment at the bottom of the tube, one dampened to catch polonium at the opening of the tube) were inserted, then the tubes were placed into a tube furnace and heated to 700°C for ½ hr to distil the polonium from the sediments. At this temperature, polonium passes easily from the sediment, through the dry wool plug and does not condense until reaching the wet wool plug outside the furnace.

After cooling, the tube was cut, and the upper part containing the damp glass wool (condenser) was digested in concentrated HNO_3 under reflux (to destroy organic material). The residue was then filtered and the filtrate boiled down and digested with two HCl treatments to remove any remaining traces of HNO_3.

The polonium was then plated from the remaining solution onto a finely polished silver disk. The disk was counted in an alpha spectrometer. ^{209}Po was identified by its 4.88 MeV alpha particle, and ^{210}Po

by its 5.305 MeV alpha particle. The ^{210}Po counts obtained from the spectrometer were compared to the ^{209}Po counts (of known activity) to determine the activity of ^{210}Po in the sediment sample.

Sediment Dating Theory

Dating of lacustrine sediments has been actively pursued for several decades (Robbins and Edgington, 1975; Matsumoto, 1975; Appleby and Oldfield, 1978; and Farmer, 1978). Sedimentation rates are derived using either the CIC (constant initial concentration of unsupported ^{210}Pb; Robbins and Edgington, 1975; Matsumoto, 1975) or the CRS (constant rate of supply; Appleby and Oldfield, 1978) model. The CIC model assumes a constant sedimentation rate over the time period in which unsupported ^{210}Pb is measured. The CRS model assumes a variable sedimentation rate. Both models assume a constant flux of unsupported ^{210}Pb to the sediment/water interface. Depth can be corrected for sediment compaction in the CIC model using sediment porosity measurements (CIC1), otherwise cumulative dry weight is used (CIC2). Sediment compaction is accounted for in the CRS model by dealing with cumulative dry weight instead of sediment depth.

The profile of ^{210}Pb in a sediment core can be described as follows:

$$A_{tx} = (A_{Uo})e^{-\lambda t} + A' \qquad (1a)$$

where A_{Tx} is the total activity of ^{210}Pb in the sample in $pCi \cdot g^{-1}$ dry wt at depth x, and of age t.

A' is the activity of ^{210}Pb supported by ^{226}Ra in $pCi \cdot g^{-1}$ dry wt (represented by constant ^{210}Po activities attained at depth),

A_{Uo} is the unsupported activity of ^{210}Pb at the sediment/water interface in $pCi \cdot g^{-1}$ dry wt,

λ is the radioactive decay constant for ^{210}Pb ($0.693/22.26\ yr^{-1} = 0.0311\ yr^{-1}$),

And since $A_{Ux} = A_{Tx} - A'$ then $A_{Ux} = (A_{Uo})e^{-\lambda t}$ (1b)

where A_{Ux} is the unsupported activity of ^{210}Pb in the sample in $pCi \cdot g^{-1}$ dry wt at depth x,

The Constant Initial Concentration (CIC) Model:

In the following derivations, equations which refer to the usage of cumulative dry weight instead of uncompacted depth in the CIC model are designated with an 'a'.

In the CIC model, uncompacted mid-depth, z, can be used instead of natural depth, x, to compensate for sediment compaction (CIC1 model). Otherwise cumulative dry weight is used (CIC2 model). The uncompacted mid-depth is calculated from uncompacted thickness (Delorme 1991).

$$t_{ui} = \{(\phi_o - \phi_i)/(1 - \phi_o)\} + (TV_i * V_q) \qquad (2)$$

where t_{ui} is the uncompacted thickness of the i^{th} sample,

ϕ_i is the porosity of the i^{th} sample expressed as a percentage,

ϕ_o is the porosity at the sediment-water interface calculated by regressing the top four sample porosities (ϕ_i) against natural mid-depth, and ϕ_o = y intercept,

TV_i is the total volume of the i^{th} sample,

V_q is the volume of a cylinder 1 cm high and surface area equal to either the inside of the core tube or the stainless steel extrusion ring, whichever is appropriate.

The CIC model assumes a constant sedimentation rate (or mass sedimentation rate) over the time period in which unsupported ^{210}Pb is measured, thus

$$t = z/S_o \qquad (3)$$

$$t = c/\omega \qquad (3a)$$

where S_o is the sedimentation rate in $cm{\cdot}yr^{-1}$ at the sediment/ water interface,

z is uncompacted mid-depth,

c is cumulative dry weight in $g{\cdot}cm^{-2}$,

ω is the mass sedimentation rate in $g{\cdot}cm^{-2}{\cdot}yr^{-1}$.

The total ^{210}Pb activity at the sediment water interface is:

$$A_{\omega} = (P/\omega) \quad (4)$$

where P is the flux of ^{210}Pb at the sediment water interface in $pCi \cdot cm^{-2} \cdot yr^{-1}$, (assumed constant).

Substituting equations (3) [and (3a)] and (4) into equation (1a) gives:

$$A_{tz} = (P/\omega)e^{-z\lambda/S_o} + A' \quad (5)$$

or

$$A_{Tx} = (P/\omega)e^{-c\lambda/\omega} + A' \quad (5a)$$

Equation (5) or [5(a)] can be simplified using natural logarithms:

$$\ln(A_{Tz} - A') = \ln(P/\omega) - (\lambda/S_o)z \quad (6)$$

$$\ln(A_{Tx} - A') = \ln(P/\omega) - (\lambda/\omega)c \quad (6a)$$

The form of the equation is $y = b + (m)\,x$

A graphical solution for P/ω (the y-intercept) and λ/S_o [or (λ/ω)] (the slope of the line) is possible from a plot of x and y {z vs $\ln(A_z - A')$} [or c vs $\ln(A_x - A')$] (see Figure 4). As λ is known, then S_o [or ω] can be calculated.

$$S_o = \lambda/\text{slope} = \lambda/(m) \quad (7)$$

$$\omega = \lambda/\text{slope} = \lambda/(m) \quad (7a)$$

When using uncompacted depth, the mass sedimentation rate ($g \cdot cm^{-2} \cdot yr^{-1}$) is represented by:

$$\omega = S_o\,(1 - \phi_o)\,\rho_s = S_i\,(1 - \phi_i)\,\rho_s \quad (8)$$

where ρ_s is the density of the solid phase of the sample (assumed constant),

S_i is the sedimentation rate ($cm \cdot yr^{-1}$) at a given uncompacted mid-depth z.

The flux at the sediment/water interface P ($pCi \cdot cm^{-2} \cdot yr^{-1}$) can be calculated from the y-intercept and mass sedimentation rate.

$$P = \omega (e^{b}) \qquad (9)$$

Using equation (6) [or (6a)] the time 't' in years since the sample was deposited is given by:

$$t = \frac{\ln (A_{Tz} - A') - \ln(P/\omega)}{(-\lambda)} = \frac{z}{S_o} \quad \text{CIC1} \qquad (10)$$

or $$t = \frac{\ln (A_{Tx} - A') - \ln(P/\omega)}{(-\lambda)} = \frac{c}{\omega} \quad \text{CIC2} \qquad (10ai)$$

which can be written as:

$$t = -\frac{1}{\lambda} \ln \frac{(A_{Tz} - A')}{A_{to}} = \frac{z}{S_o} \text{ or } = \frac{c}{\omega} \qquad (10aii)$$

The uncompacted mid-depth (cm) divided by the sedimentation rate ($cm \cdot yr^{-1}$) [or cumulative dry weight, ($g \cdot cm^{-2}$) divided by mass sedimentation rate ($g \cdot cm^{-2} \cdot yr^{-1}$)] gives t.

The Constant Rate of Supply (CRS) Model:

Since the CRS model assumes a constant rate of supply, then

$$P = A_{Ui} * \omega_t \qquad (11)$$

where P is the flux of ^{210}Pb at the sediment water interface in $pCi \cdot cm^{-2} \cdot yr^{-1}$, (assumed constant)

A_{Ui} is the initial activity of unsupported ^{210}Pb in sediment of age t

ω_t is the dry Mass Sedimentation Rate ($g \cdot cm^{-2} \cdot yr^{-1}$) at time t.

Sediment laid down during time period δt occupies a layer of thickness (δx):

$$\delta x = \frac{\omega_t}{\rho_x} \delta t \qquad (12)$$

were ρ_x is the dry mass/unit wet volume of the sample ($g \cdot cm^{-3}$) at depth x.

$$\rho_x = \frac{d\omega}{dx} \qquad (13)$$

The rate of change of depth is

$$x' = \frac{\omega}{\rho_x} \qquad (14)$$

where ' denotes differentiation with regards to t.

and $$x' \rho_x = \omega = x'_o \rho_o \qquad (15)$$

Equation (15) combines with (1b) to give

$$x' \rho_x A_{Ux} = x'_o \rho_o (A_{Uo}) e^{-\lambda t} \qquad (16)$$

Let $$B(x) = \int_x^\infty \rho_x * A_{Ux} \, dx = \int_x^\infty A_{Ux} \, d\omega \qquad (17)$$

represent the total residual or cumulative unsupported ^{210}Pb beneath sediments of depth x,

and $$B(0) = \int_0^\infty \rho_o * A_{Uo} \, dx = \int_0^\infty A_{Uo} \, d\omega \qquad (18)$$

represent the total residual unsupported ^{210}Pb in the sediment column, then

$$B(x) = B(0) e^{-\lambda t} \qquad (19)$$

The age of layer at depth x is thus:

$$t = -\frac{1}{\lambda} \ln \frac{B(x)}{B(0)} \qquad (20)$$

where B(x) and B(0) are calculated by direct numerical integration of the ^{210}Pb profile (the plot of unsupported activity versus cumulative dry weight).

The mass sedimentation rate is calculated by dividing the change in the mid-sample cumulative dry weight by the difference of time in years for the sample analysed.

The mean ^{210}Pb supply rate (flux) is calculated from

$$P = \lambda B(0) \qquad (21)$$

Quality Assurance/Quality Control

Quality Assurance: Collection and Preparation of Core Samples

The samples for core 214 were collected by divers using a benthos coring tube. The cores were stored for over a year before extrusion. The topmost two samples were scooped out before the core was cut in half lengthwise. The remaining samples were sliced, then scooped out of the coring tube and placed in plastic vials. This is an imprecise method with inaccuracies involved in cutting the core tube as well as slicing and scooping. The extent of the inaccuracies is unknown.

The samples were freeze-dried using a standard procedure. Minimum loss of water from each sample was achieved by keeping tight lids on the vials before weighing and freeze drying, however water loss may have occurred during sampling as the core was exposed to the air for a period of time. An attempt was made to minimize this exposure time by working as quickly as possible. The amount of water loss during the exposure time is unknown..

Quality Control: Contamination and Method Checks

Blanks (no sample, no spike), were run through the same analytical procedures as samples, to determine if there was contamination from analytical reagents. Blanks, prepared at the same time as

the sediment samples, exhibited a background activity of 0.03 dpm when run in all detectors, an activity comparable to empty sample holders.

Yield tracer solutions (no sediment sample) were also run through the analytical procedure. No counts above background were detectable in the ^{210}Po region of the spectra for disks prepared using only the spike (no sample), indicating no polonium (^{210}Po) contamination in the analyses from spike solutions.

RESULTS

Table 1 lists the ^{210}Po activities for the 19 samples prepared for core 214. Figure 3 depicts the ^{210}Po activity profile with depth and cumulative dry weight. The symbols used in figure 3 indicate which detector was used during sample analysis. X's represent detector 3, triangles represent detector 2, and squares represent detector 1.

Table 1. Activity of ^{210}Po in Core 214 Sediment.

Sample	Cum. Dry Wt., $g\,cm^{-2}$	Uncompacted Mid Depth, cm	^{210}Po, $dpm\,g^{-1}$		Sample	Cum. Dry Wt., $g\,cm^{-2}$	Uncompacted Mid Depth, cm	^{210}Po, $dpm\,g^{-1}$
1	0.34	0.68	9.46		22	10.53	43.87	5.84
3	1.17	4.05	9.98		24	11.77	48.95	4.91
5	2.16	7.93	11.53		24R	11.77	48.95	4.84
7	2.90	11.33	11.05		24R2	11.77	48.95	5.08
10	4.12	16.62	9.80		26	12.98	54.12	4.86
12	5.11	20.49	7.40		28	14.07	59.17	5.80
14	6.27	25.38	7.08		30	15.20	63.99	4.79
16	7.36	30.01	6.82		35	17.94	75.78	5.35
18	8.35	34.50	6.88		40	22.22	90.15	2.61
20	9.45	39.03	6.18					

Reproducibility of Results

One slice from core 214 was chosen to have the analysis for ^{210}Po repeated. Sample 24 gave a mean activity of 4.94 ± 0.12. The ^{210}Po activities are given in Table 1.

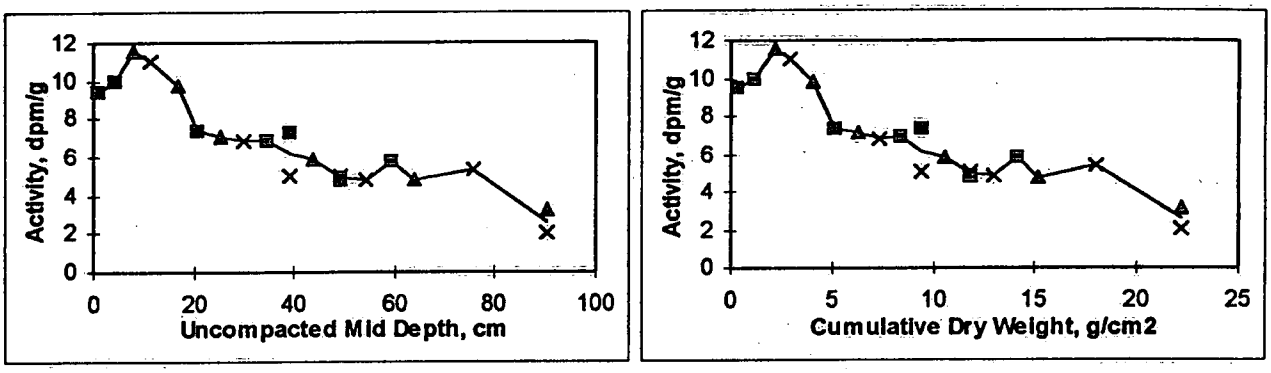

Figure 3. Distribution of Total ^{210}Po activity in $dpm \cdot g^{-1}$ in relation to uncompacted mid-depth and cumulative dry weight for core 214.

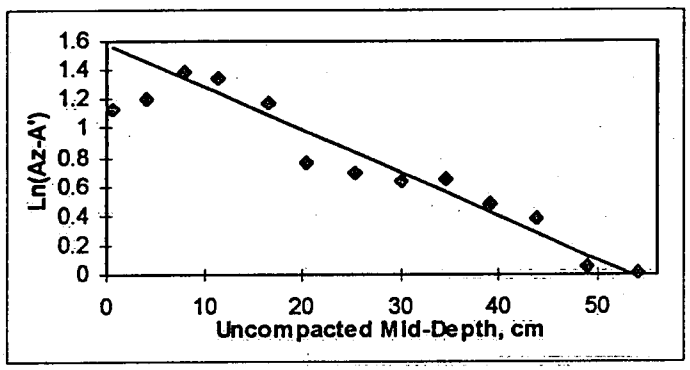

Figure 4. The distribution of uncompacted mid-depth against $\ln(A_z - A')$ for core 214. The y intercept of the regression line = 1.5811, the slope = -0.0295.

^{210}Pb Analysis of core 214 using the CIC model.

For the first CIC model (CIC1), the unsupported activity is plotted against uncompacted mid-depth (Figure 4) using the expanded equation (6). Based on the graphical solution, the y-intercept is $\ln(P/\omega) = 1.5811$ and the slope of the line (λ/S_o) is -0.0295 (see Appendix D). Samples 3 to 13 were used to calculate an average sedimentation rate of 1.05 $cm \cdot yr^{-1}$, an average mass sedimentation rate of 0.26 $g cm^{-2} yr^{-1}$ and a flux of 1.25 $pCi\, cm^{-2} yr^{-1}$. The mean dates calculated for each core section, based on a division of the uncompacted mid-depth by the sedimentation rate (equation 3), are given in Appendix G. The '±' values are two standard deviations based on data calculated for the top, bottom, and mid-depth of the sample.

For the second CIC model (CIC2), the unsupported activity is plotted against cumulative dry weight (Figure 5) using the expanded equation (6a). Based on the graphical solution, the y-intercept is $\ln(P/\omega) = 1.5918$ and the slope of the line (λ/ω) is -0.1271 (see Appendix E). Samples 3 to 13 were used to calculate an average mass sedimentation rate of 0.25 $g{\cdot}cm^{-2}{\cdot}yr^{-1}$ and a flux of 1.20 $pCi{\cdot}cm^{-2}{\cdot}yr^{-1}$. The dates calculated for each core section, based on a division of the cumulative dry weight by the mass sedimentation rate (equation 3a) are given in Appendix G. The '±' values are two standard deviations based on data calculated for the top, bottom, and mid-section of the sample.

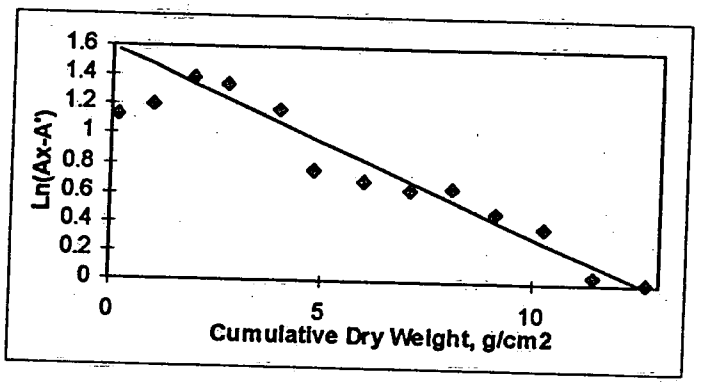

Figure 5. The distribution of cumulative dry weight against $\ln(A_x - A')$ for core 214. The y intercept of the regression line = 1.5918, the slope = -0.1271.

Ideally, the CIC1 and CIC2 models should give almost identical results. A comparison of the mass sedimentation for this core shows excellent agreement. The calculated atmospheric flux rates are also in agreement.

A difference in the mass sedimentation rates or atmospheric fluxes determined from the CIC1 and CIC2 models may indicate a problem in the calculation of uncompacted mid-depth. It may indicate a change in lithology that was not completely accounted for by porosity or specific gravity measurements.

^{210}Pb Analysis of core 214 using the CRS model.

For the CRS model, the unsupported activity is plotted against cumulative dry weight (Figure 3). The profile is integrated to determine B(0) and B(x) and calculate time (see Appendix F) according to equation 20. Since not all samples were analysed for ^{210}Pb activity, a multiple regression analysis was performed to obtain the dates for each core section as given in Appendix G. Samples 1 to 16 were used in this example to calculate an average mass sedimentation rate of 0.26 ± 0.06 $g{\cdot}cm^{-2}{\cdot}yr^{-1}$ and flux

of 1.16 $pCi{\cdot}cm^{-2}{\cdot}yr^{-1}$. The variation in mass sedimentation rate in core 214 is illustrated in figure 6. Slight changes (decrease) in mass sedimentation rate between 2 and 5 $g{\cdot}cm^{-2}$ in the upper core coincides with one zone of changing porosity (Figure 2a). The other fluctuations in accumulation rate do no coincide with any obvious changes in porosity.

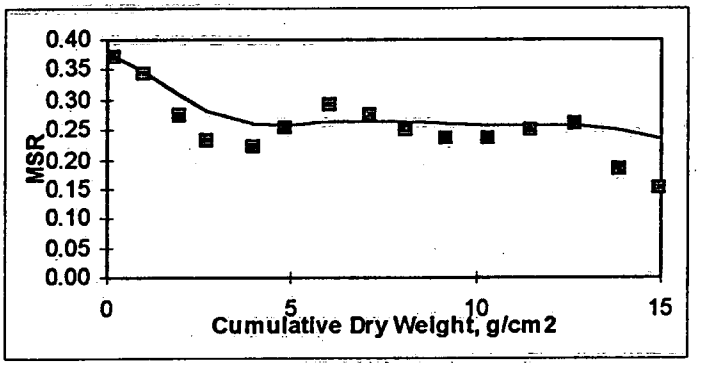

Figure 6. Plot of mass sedimentation rate versus cumulative dry weight for core 214. Points represent mass sedimentation rates determined from integrated area defined by activity and cumulative dry weight for the sample, the line represents the running mean of the mass sedimentation rate.

Comparison of CIC and CRS ^{210}Pb Analysis of Core 214.

Table 2 lists mass sedimentation and atmospheric flux rates as calculated from the CIC and CRS models. The mass sedimentation rates are in excellent agreement. The three calculated atmospheric flux rates also agree well.

The year corresponding to individual core sections (Appendix G) as determined by the CIC and CRS models are plotted against cumulative dry weight in Figure 7. Figure 7 shows good agreement between the chronology of the two CIC models and the CRS model.

Table 2. Summary of Mass Sedimentation Rate and Atmospheric Flux.

Model	Average Mass Sedimentation Rate, $g{\cdot}cm^{-2}{\cdot}yr^{-1}$	Calculated Atmospheric Flux $pCi{\cdot}cm^{-2}{\cdot}yr^{-1}$
CIC1	0.26	1.25
CIC2	0.25	1.20
CRS	0.26 + 0.06*	1.16

* Based on incremental mass sedimentation rates (Appendix F)

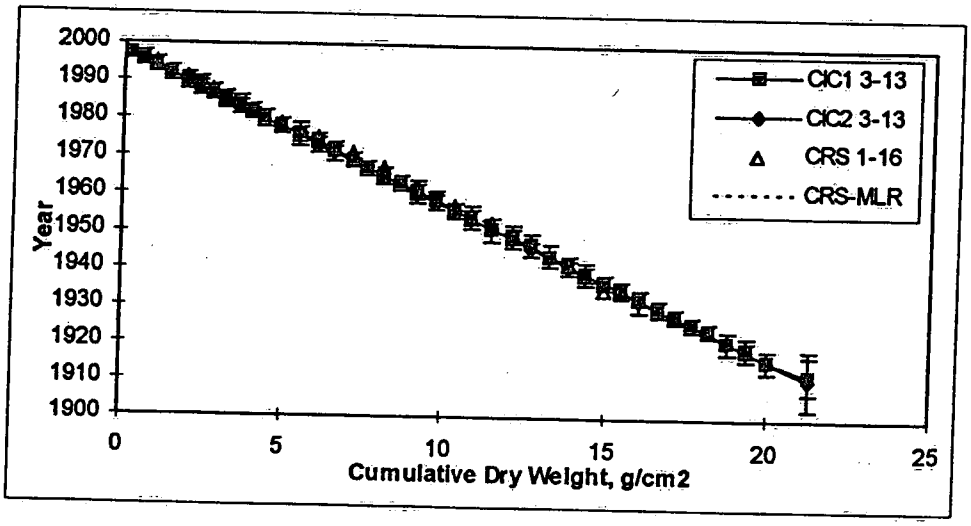

Figure 7. Plot of the Year determined from CIC (squares and diamonds)/CRS (triangles) models versus cumulative dry weight for core 214.

Sediment focusing in the St. Lawrence River as evidenced by Core 214.

Sediment focusing (Likens and Davis, 1975) is a phenomenon whereby fine sediment is transported from shallow areas to deeper areas through resuspension and settling. Sediment distribution is influenced by water body properties such as mixing depth in the water column, wave and current shear stress and sediment cohesiveness as well as physical variables such as exposure (circular integral of fetch), slope and sediment texture (water content and organic content) (Blais and Kalff, 1995). Hilton et al. (1986) presented evidence for 10 mechanisms whereby sediment is distributed in small lakes, with active sediment focusing processes being the dominant distribution mechanism. Hakanson (1977) divided lake bottoms into three zones (the erosional, the transportation, and the accumulation zones) according to the differences in their potential for resuspension. Rowan et al. (1992) developed a model for predicting the extent of the zone of erosion. Hilton (1985) presented a conceptual model for predicting the overall occurrence of sediment focusing and redistribution in small lakes. Blais and Kalff (1995) used Pb as a geochemical tracer to track sediment focusing patterns in 12 lakes. They produced the first general model for sediment focusing patterns.

A focusing factor (FF) reflects the process of sediment focusing at a particular site. Focusing factors

can be determined through a comparison of the unsupported ^{210}Pb inventory in the sediment column at a site to that deposited from the atmosphere (Simcik et al. 1996).

$$FF = I_u / I_a \tag{22}$$

where FF is the focusing factor,

I_u is the unsupported ^{210}Pb inventory in $pCi \cdot cm^{-2}$,

and I_a is the atmospheric ^{210}Pb inventory in $pCi \cdot cm^{-2}$.

An alternate method is through comparison of flux calculated from unsupported ^{210}Pb activity profile and the actual atmospheric flux as measured from atmospheric fallout or estimated from soil profiles.

$$FF = P / F_a \tag{23}$$

where P is the flux at the sediment/water interface in $pCi \cdot cm^{-2} \cdot yr^{-1}$,

and F_a is the atmospheric flux in $pCi \cdot cm^{-2} \cdot yr^{-1}$.

Depositional environments exhibit focusing factors greater than 1. Erosional environments with intermittent sediment accumulation exhibit focusing factors less than 1.

The CIC and CRS models used for the determination of sedimentation rate and chronology provide the flux calculated from the sediment profile (P) as required by equation (23). These values are given in Table 2. The CRS model includes an integration of the activity profile which provides a value for the unsupported ^{210}Pb inventory as required by equation (22) (see appendix G).

Atmospheric ^{210}Pb inventory and/or atmospheric flux values for some sites have been reported in the literature. Klusek (1978) determined the ^{210}Pb inventory of soil at Rhinebeck, NY, to be 5.70 $kBq \cdot m^{-2}$ (or 15.5 $pCi \cdot cm^{-2}$). This site is southeast of the Adirondack lakes of New York. It is assumed to be fairly representative of the this part of the northeast U.S.A. (Graustein and Turekian, 1986). Wong et al. used this value as the atmospheric ^{210}Pb inventory in their calculation of focusing factors in various basins of Lake Ontario. Simick et al. (1996) also used this value when calculating focusing factors for sediments in Lake Michigan. If the value 15.5 $pCi \cdot cm^{-2}$ is used along with the value for atmospheric ^{210}Pb inventory as determined by the CRS model for core 214 (37.23 $pCi \cdot cm^{-2}$) , equation

(22) produces a focusing factor of 2.40 (Table 3).

Urban et al. (1990) relate the net atmospheric flux of ^{210}Pb to peat under the assumption of steady state conditions to the unsupported ^{210}Pb inventory by the following equation:

$$F_a = \lambda I_u \qquad (24)$$

where F_a is the net flux of ^{210}Pb to peat in $pCi \cdot cm^{-2} yr^{-1}$,

λ is the decay constant for ^{210}Pb ($0.0311\ yr^{-1}$)

and I_u is the unsupported ^{210}Pb inventory in $pCi \cdot cm^{-2}$

Under steady state conditions, an inventory of 15.5 $pCi \cdot cm^{-2}$ would arise from a net flux of 0.48205 $pCi \cdot cm^{-2} yr^{-1}$. The CIC and CRS model output flux rates can be compared to this net flux using equation (23). The resulting focusing factors are given in Table 3.

Table 3: Focusing factors calculated from Model output data.

Model	Calculated Flux Rate $pCi \cdot cm^{-2} yr^{-1}$	Unsupported ^{210}Pb Inventory $pCi \cdot cm^{-2}$	Focusing Factor
CIC1	1.25		2.59
CIC2	1.20		2.49
CRS	1.16		2.41
CRS		37.23	2.40

REFERENCES

Appleby, P.G. and F. Oldfield. 1978. The calculation of ^{210}Pb dates assuming a constant rate of supply of unsupported ^{210}Pb to the sediment. Catena 5:1-8.

Blais, J.M. and J. Kalff. 1995. The influence of lake morphology on sediment focusing. Limnol. Oceanogr. 40(3):582-588.

Delorme, L.D. 1991. The preparation of lacustrine sediment samples from cores for use in dating and paleolimnology. National Water Research Institute, Burlington, Ontario, Contribution 92-188, 18p.

Eakins, J.D. and R.T. Morrison. 1978. A new procedure for determination of lead-210 in lake and marine sediments. International Journal of Applied Radiation and Isotopes 29:531-536.

Farmer, J.G. 1978. The determination of sedimentation rates in Lake Ontario using the ^{210}Pb dating method. Canadian Journal of Earth Sciences 15:431-437.

Graustein, W.C. and K.K. Turekain (1986). 210Pb and 137Cs in air and soils measure the rate and vertical profile of aerosol scavenging. J. Geophys Res 91: 14355-14366.

Hakanson, L. 1977. The influence of wind, fetch and water depth on the distribution of sediments in Lake Vanern, Sweden. Can. J. Earth Sci. 14:397-412.

Hilton, J. 1985. A conceptual framework for predicting the occurrence of sediment focusing and sediment redistribution in small lakes. Limnol. Oceanogr. 30(6):1131-1143.

Hilton, J., J.P. Lishman, and P.V. Allen. 1986. The dominant process of sediment distribution and focusing in a small, eutrophic, monomictic lake. Limnol. Oceanogr. 31(1):125-133.

Klusek, C.S. (1987). Soil Sampling intercomparison. U.S.Dept. Energy Report, EML-501, New York, 201 pp.

Likens, G.E. and M.B. Davis. 1975. Post-glacial history of Mirror Lake and its watershed in New Hampshore, U.S.A., and initial report. Int. Ver. Theor. Angew. Limnol. Verh. 19:982-993.

Matsumoto, E. 1975. ^{210}Pb geochronology of sediments from Lake Shinji. Geochemical Journal 9:167-172.

Micromeritics 1992. Automated Accupyc pycnometer 1330, for determining skeletal density and volume of powders, porous materials, and irregularly shaped solid objects. Operators Manual V2.01, Micromeritics Instrument Corporation, Norcross, Georgia.

Oldfield, F. and P.G. Appleby. 1984. Empirical testing of ^{210}Pb dating models for lake sediments IN Lake Sediments and Environmental History (Eds. E.Y. Harworth and J.W.G. Lund). University of Minnesota Press, Minneapolis. pp 93-124.

Robbins, J.A. and D.N. Edgington. 1975. Determination of recent sedimentation rates in Lake Michigan using Pb-210 and Cs-137. Geochimica et Cosmochimica Acta 39:285-304.

Rowan, D.J., J. Kalff and J.B. Rasmussen. 1992. Estimating the mud deposition boundary depth in lakes from wave theory. Can. J. Fish. Aquat. Sci. 49:2490-2497.

Simcik, M.F., S.J. Eisenreich, K.A. Golden, S.P. Liu, E. Lipiatou, D.L. Swackhamer and D.T. Long. 1996. Atmospheric loading of polycyclic aromatic hydrocarbons to Lake Michigan as recorded in sediments. Environ. Sci. Technol. 40:3039-3046.

Turner, L.J. 1999a. ^{210}Pb analysis of sediments from the St. Lawrence River (Station 109, Core 212), Ontario. National Water Research Institute, Burlington, Ontario. NWRI Technical Report PB99-4, 23p

Turner, L.J. 1999b. ^{210}Pb analysis of sediments from the St. Lawrence River (Station 166, Core 213), Ontario. National Water Research Institute, Burlington, Ontario. NWRI Technical Report PB99-5, 25p

Turner, L.J. 1996a. ^{210}Pb dating of riverine sediments from the St. Lawrence River (Core 079, Station 3-1), Ontario. National Water Research Institute, Burlington, Ontario. NWRI Contribution 96-03, 28p.

Turner, L.J. 1996b. ^{210}Pb dating of sediments from the St. Lawrence River (Core 087, Station TCT1), Ontario. National Water Research Institute, Burlington, Ontario. NWRI Contribution 96-28, 27p.

Turner, L.J. 1996c. ^{210}Pb dating of sediments from Lake St. Lawrence (Core 088, Station LSL), Ontario. National Water Research Institute, Burlington, Ontario. NWRI Contribution 96-29, 27p

Turner, L.J. 1996d. ^{210}Pb dating of sediments the St. Lawrence River (Core 091, Station PILON), Ontario. National Water Research Institute, Burlington, Ontario. NWRI Contribution 96-30, 27p

Turner, L.J. 1996e. ^{210}Pb dating of sediments from Lake St. Francis (Core 092, Station LSF5), Ontario. National Water Research Institute, Burlington, Ontario. NWRI Contribution 96-31, 27p

Turner, L.J. 1996f. ^{210}Pb dating of sediments from Lake St. Francis (Core 089, Station LSFN), Ontario. National Water Research Institute, Burlington, Ontario. NWRI Contribution 96-34, 27p

Turner, L.J. 1996g. ^{210}Pb dating of sediments from Lake St. Francis (Core 090, Station LSFM), Ontario. National Water Research Institute, Burlington, Ontario. NWRI Contribution 96-35, 24p

Turner, L.J. 1990. Laboratory determination of ^{210}Pb - ^{210}Po using alpha spectrometry: Second Edition. NWRI Tech. Note LRB-90-TN-07, Burlington, Ontario, 63p.

Wong, C.S., G.Sanders, D.R.Engstrom, D.T.Long, D.L.Swackhamer & S.J.Eisenreich 1995. Accumulation, inventory, and diagenesis of chlorinated hydrocarbons in Lake Ontario sediments. Env.Sci.Technol. 29:2661-2672.

Appendix A: Wet and dry weights for core 214.

Sample Number	Wet Weight	Dry Weight		Sample Number	Wet Weight	Dry Weight
1	44.554	11.568		21	44.042	19.578
2	49.256	16.429		22	38.728	17.206
3	32.274	11.936		23	44.038	20.624
4	45.496	17.746		24	46.594	21.810
5	46.260	16.086		25	47.656	21.216
6	35.654	12.322		26	41.374	20.070
7	36.356	13.142		27	46.666	21.362
8	45.124	16.194		28	35.980	16.058
9	41.020	14.226		29	45.710	20.554
10	32.010	11.192		30	39.976	17.976
11	39.236	14.772		31	42.424	18.950
12	43.092	19.284		32	51.278	22.628
13	49.564	21.942		33	40.296	17.584
14	40.292	17.634		34	39.104	16.870
15	46.438	19.706		35	42.714	17.882
16	40.948	17.718		36	42.162	18.454
17	35.762	15.616		37	47.142	22.134
18	42.530	18.226		38	35.376	17.792
19	41.224	16.892		39	45.016	24.234
20	46.360	20.828		40	107.460	63.912

Appendix B: Calculation of porosity and uncompacted depths given sample wet and dry weights, (Delorme, 1991) and specific gravity for core 214.

Sample Number	Wet Wt. g	Dry Wt. g	Cumm. Dry Wt g/cm2	Water Cont. cm3	Sed. Vol. cm3	Total Vol. cm3	Comp. Thick cm	Comp. Depth cm	Comp. Mid-pt cm	Sample Poros. %	Uncomp Thick. cm	Uncomp Depth cm	Uncomp Mid-pt cm	Time B.P. Years
1	44.55	11.57	0.34	32.99	4.47	37.45	1.09	1.09	0.55	88.07	1.35	1.35	0.68	0
2	49.26	16.43	0.82	32.83	6.35	39.17	1.15	2.24	1.67	83.80	1.86	3.21	2.28	2
3	32.27	11.94	1.17	20.34	4.61	24.95	0.73	2.97	2.60	81.52	1.68	4.89	4.05	3
4	45.50	17.75	1.69	27.75	6.85	34.60	1.01	3.98	3.47	80.19	2.10	6.99	5.94	5
5	46.26	16.09	2.16	30.17	6.21	36.39	1.06	5.04	4.51	82.92	1.87	8.86	7.93	7
6	35.65	12.32	2.52	23.33	4.76	28.09	0.82	5.87	5.45	83.06	1.61	10.47	9.67	9
7	36.36	13.14	2.90	23.21	5.08	28.29	0.83	6.69	6.28	82.06	1.72	12.19	11.33	10
8	45.12	16.19	3.37	28.93	6.26	35.19	1.03	7.72	7.21	82.22	1.91	14.10	13.15	12
9	41.02	14.23	3.79	26.79	5.49	32.29	0.94	8.66	8.19	82.98	1.74	15.84	14.97	14
10	32.01	11.19	4.12	20.82	4.32	25.14	0.73	9.40	9.03	82.80	1.55	17.39	16.62	15
11	39.24	14.77	4.55	24.46	5.71	30.17	0.88	10.28	9.84	81.09	1.88	19.27	18.33	17
12	43.09	19.28	5.11	23.81	7.45	31.26	0.91	11.19	10.74	76.17	2.43	21.70	20.49	19
13	49.56	21.94	5.75	27.62	8.48	36.10	1.06	12.25	11.72	76.52	2.53	24.23	22.97	21
14	40.29	17.63	6.27	22.66	6.81	29.47	0.86	13.11	12.68	76.89	2.30	26.53	25.38	24
15	46.44	19.71	6.84	26.73	7.61	34.34	1.00	14.11	13.61	77.84	2.34	28.87	27.70	26
16	40.95	17.72	7.36	23.23	6.84	30.07	0.88	14.99	14.55	77.24	2.28	31.15	30.01	28
17	35.76	15.62	7.82	20.15	6.03	26.18	0.77	15.76	15.38	76.96	2.20	33.35	32.25	30
18	42.53	18.23	8.35	24.30	7.04	31.34	0.92	16.68	16.22	77.54	2.29	35.64	34.50	32
19	41.22	16.89	8.85	24.33	6.52	30.86	0.90	17.58	17.13	78.85	2.13	37.77	36.71	34
20	46.36	20.83	9.45	25.53	8.04	33.58	0.98	18.56	18.07	76.04	2.51	40.28	39.03	37
21	44.04	19.58	10.03	24.46	7.56	32.03	0.94	19.49	19.03	76.39	2.43	42.71	41.50	39
22	38.73	17.21	10.53	21.52	6.65	28.17	0.82	20.32	19.91	76.41	2.31	45.02	43.87	41
23	44.04	20.62	11.13	23.41	7.97	31.38	0.92	21.24	20.78	74.61	2.60	47.62	46.32	43
24	46.59	21.81	11.77	24.78	8.42	33.21	0.97	22.21	21.72	74.63	2.65	50.27	48.95	46
25	47.66	21.22	12.39	26.44	8.19	34.63	1.01	23.22	22.71	76.34	2.51	52.78	51.53	48
26	41.37	20.07	12.98	21.30	7.75	29.06	0.85	24.07	23.64	73.32	2.67	55.45	54.12	51
27	46.67	21.36	13.60	25.30	8.25	33.56	0.98	25.05	24.56	75.41	2.58	58.03	56.74	53
28	35.98	16.06	14.07	19.92	6.20	26.12	0.76	25.81	25.43	76.26	2.27	60.30	59.17	56
29	45.71	20.55	14.67	25.16	7.94	33.10	0.97	26.78	26.30	76.01	2.50	62.80	61.55	58
30	39.98	17.98	15.20	22.00	6.94	28.94	0.85	27.63	27.20	76.01	2.38	65.18	63.99	60
31	42.42	18.95	15.75	23.47	7.32	30.79	0.90	28.53	28.08	76.23	2.41	67.59	66.39	63
32	51.28	22.63	16.41	28.65	8.74	37.39	1.09	29.62	29.07	76.62	2.56	70.15	68.87	65
33	40.30	17.58	16.93	22.71	6.79	29.50	0.86	30.48	30.05	76.98	2.29	72.44	71.30	67
34	39.10	16.87	17.42	22.23	6.52	28.75	0.84	31.32	30.90	77.34	2.23	74.67	73.56	69
35	42.71	17.88	17.94	24.83	6.91	31.74	0.93	32.25	31.79	78.24	2.22	76.89	75.78	71
36	42.16	18.45	18.48	23.71	7.13	30.84	0.90	33.15	32.70	76.88	2.34	79.23	78.06	74
37	47.14	22.13	19.13	25.01	8.55	33.56	0.98	34.13	33.64	74.52	2.67	81.90	80.57	76
38	35.38	17.79	19.65	17.58	6.87	24.46	0.71	34.85	34.49	71.90	2.68	84.58	83.24	78
39	45.02	24.23	20.36	20.78	9.36	30.14	0.88	35.73	35.29	68.95	3.16	87.74	86.16	81
40	107.46	63.91	22.22	43.55	24.69	68.23	1.99	37.72	36.72	63.82	4.81	92.55	90.15	85

Appendix C. Specific gravity determination.

The specific gravities ($g \cdot cm^{-3}$) of Core 214 sediments were determined using an automated Accupyc pycnometer (Micromeritics, 1992).

Sample	No. Of Tests	Uncompacted Mid Depth	Specific Gravity	Mean
1	5	0.68	2.547 ± 0.003	
10	5	16.62	2.574 ± 0.002	
20	5	39.03	2.591 ± 0.001	
30	5	63.99	2.586 ± 0.003	
40	5	90.15	2.647 ± 0.002	2.589 ± 0.037

Appendix D. Lead Sedimentation Rate Analysis, CIC1 Model.

$\ln (A - A') = \ln (4.860) - 0.029 (Z)$ $R = -0.975$
where $(A - A')$ = unsupported ^{210}Pb in $pCi \cdot g^{-1}$,
and Z = uncompacted depth in cm.
based on data from lines 3 to 13
Specific Gravity = 2.589 $g \cdot cm^{-3}$ $P/\omega = 4.860$ $\omega = 0.257$
The initial porosity at the sediment/water interface is 90.58
Atmospheric flux rate at the time of collection 1997.884 is 2.773 $dpm \cdot cm^{-2} \cdot yr^{-1}$ or 1.249 $pCi \cdot cm^{-2} \cdot yr^{-1}$
Supported ^{226}Ra activity = 1.176 $pCi \cdot g^{-1}$ or 2.610 $dpm \cdot g^{-1}$
Sedimentation Rate = 1.054 $cm \cdot yr^{-1}$
Mass Sedimentation Rate = 0.257 $g \cdot cm^{-2} \cdot yr^{-1}$

Summary of ^{210}Pb Analyses							
Uncomp Depth cm.	Porosity	Total ^{210}Pb $dpm \cdot g^{-1}$	Total ^{210}Pb $pCi \cdot g^{-1}$	Unsupp ^{210}Pb $dpm \cdot g^{-1}$	Unsupp ^{210}Pb $pCi \cdot g^{-1}$	Sed. Rate $cm \cdot yr^{-1}$	Years (*)
7.93	0.8292	11.53	5.19	8.92	4.02	1.025	1990
11.33	0.8206	11.05	4.98	8.44	3.80	1.147	1988
16.62	0.8280	9.80	4.14	7.19	3.24	1.226	1984
20.49	0.7617	7.40	3.33	4.79	2.16	1.112	1979
25.38	0.7689	7.08	3.19	4.47	2.01	1.149	1976
30.01	0.7724	6.82	3.07	4.21	1.90	1.130	1971
34.50	0.7754	6.88	3.10	4.27	1.92	1.100	1967
39.03	0.7604	6.18	2.78	3.57	1.61	1.061	1961
43.87	0.7641	5.84	2.63	3.23	1.46	1.186	1961
48.95	0.7463	4.94	2.23	2.33	1.05	1.069	1952
54.12	0.7332	4.86	2.19	2.25	1.01	1.169	1952
59.17	0.7626	5.80	2.63	3.19	1.44	1.249	1951
63.99	0.7601	4.79	2.16	2.18	0.98	1.159	1943
75.78	0.7824	5.35	2.41	2.74	1.23	1.089	1928
90.15	0.6382	2.61	1.18	0.00	0.00	0.663	1862

(*) Year calculated using the sedimentation rate of the sample

Appendix E. Lead Sedimentation Rate Analysis, CIC2 Model.

$\ln (A - A') = \ln (4.913) - 0.127 (X)$ $R = -0.975$
where $(A - A')$ = unsupported ^{210}Pb in $pCi \cdot g^{-1}$,
and X = cumulative dry weight in $g \cdot cm^{-2}$
based on data from lines 3 to 13
Specific Gravity = 2.589 $g \cdot cm^{-3}$ $P/\omega = 4.913$ $\omega = 0.245$
The initial porosity at the sediment/water interface is 90.58
Atmospheric flux rate at the time of collection 1997.884 is 2.672 $dpm \cdot cm^{-2} \cdot yr^{-1}$ or 1.204 $pCi \cdot cm^{-2} \cdot yr^{-1}$
Supported ^{226}Ra activity = 1.176 $pCi \cdot g^{-1}$ or 2.610 $dpm \cdot g^{-1}$
Mass Sedimentation Rate = 0.245 $g \cdot cm^{-2} \cdot yr^{-1}$

Summary of ^{210}Pb Analyses						
Mid-Sample Cum. Dry Wt. $g \cdot cm^{-2}$	Porosity	Total ^{210}Pb $dpm \cdot g^{-1}$	Total ^{210}Pb $pCi \cdot g^{-1}$	Unsupp ^{210}Pb $dpm \cdot g^{-1}$	Unsupp ^{210}Pb $pCi \cdot g^{-1}$	Years (*)
1.93	0.8292	11.53	5.194	8.92	4.018	1990
2.71	0.8206	11.05	4.977	8.44	3.802	1987
3.95	0.8280	9.80	4.414	7.19	3.239	1982
4.83	0.7617	7.40	3.333	4.79	2.158	1978
6.01	0.7689	7.08	3.189	4.47	2.014	1973
7.10	0.7724	6.82	3.072	4.21	1.896	1969
8.09	0.7754	6.88	3.099	4.27	1.924	1965
9.15	0.7604	6.18	2.784	3.57	1.608	1961
10.28	0.7641	5.84	2.631	3.23	1.455	1956
11.45	0.7463	4.94	2.225	2.33	1.050	1951
12.68	0.7332	4.86	2.189	2.25	1.014	1946
13.84	0.7626	5.80	2.613	3.19	1.437	1941
14.93	0.7601	4.79	2.158	2.18	0.982	1937
17.68	0.7824	5.35	2.410	2.74	1.234	1926
21.29	0.6382	2.61	1.176	0.00	0.00	1911

(*) Year calculated using the mass sedimentation rate of the sample

Appendix F. Lead Sedimentation Rate Analysis, CRS Model.

Uncompacted Mid-Pt., cm	Cum. Dry Wt., $g{\cdot}cm^{-2}$	Mid Section Cum. Dry Wt., $g{\cdot}cm^{-2}$	Unsup. Activity $pCi{\cdot}g^{-1}$	Area $pCi{\cdot}cm^{-2}$	Cum. Area $pCi{\cdot}cm^{-2}$	Time, B.P. Years	Cum Avg Mass Sed Rate, $g{\cdot}cm^{-2}{\cdot}yr^{-1}$	Date	Mass Sed Rate $g{\cdot}cm^{-2}{\cdot}yr^{-1}$
0.68	0.34	0.17	3.086	0.525	0.525	0.46	0.373	1997	0.373
4.05	1.17	1.00	3.086	2.642	3.167	2.86	0.348	1995	0.344
7.93	2.16	1.93	3.320	3.412	6.579	6.25	0.308	1991	0.274
11.33	2.90	2.71	4.018	3.069	9.648	9.64	0.281	1988	0.232
16.62	4.12	3.95	3.802	4.383	14.031	15.20	0.260	1982	0.244
20.49	5.11	4.83	3.239	2.361	16.392	18.64	0.259	1979	0.254
25.38	6.27	6.01	2.158	2.461	18.853	22.68	0.265	1975	0.292
30.01	7.36	7.10	2.014	2.131	20.984	26.64	0.266	1971	0.275
34.50	8.35	8.09	1.896	1.881	22.866	30.60	0.264	1967	0.249
39.03	9.45	9.15	1.924	1.881	24.746	35.11	0.261	1962	0.236
43.87	10.53	10.28	1.608	1.731	26.477	39.90	0.258	1957	0.236
48.95	11.77	11.45	1.455	1.465	27.942	44.61	0.257	1953	0.249
54.12	12.98	12.68	1.050	1.274	29.216	49.35	0.257	1948	0.260
59.17	14.07	13.84	1.014	1.409	30.626	55.57	0.249	1942	0.185
63.99	15.20	14.93	1.437	1.331	31.956	62.80	0.238	1935	0.152
								Mean	0.256
								StdDev	0.055

Based on data from lines 1 to 16. Unsupported ^{210}Pb inventory = 37.226 $pCi{\cdot}cm^{-2}$.
Atmospheric flux rate at the time of collection 1997.884 is 1.16 $pCi{\cdot}cm^{-2}{\cdot}yr^{-1}$

Appendix G. Mean date calculated for each core slice.

Sample	Uncompacted Mid Depth cm	Cumulative Dry Weight $g \cdot cm^{-2}$	Cumulative Dry Weight Mid Sample	CIC1 Year	CIC2 Year	CRS Year	CRS-MLR Year*
1	0.68	0.34	0.17	1997 ± 1	1997 ± 1	1997	1998
2	2.28	0.82	0.58	1996 ± 2	1996 ± 2		1996
3	4.05	1.17	1.00	1994 ± 2	1994 ± 2	1995	1994
4	5.94	1.69	1.43	1992 ± 2	1992 ± 2		1993
5	7.93	2.16	1.93	1990 ± 2	1990 ± 2	1991	1991
6	9.67	2.52	2.34	1989 ± 2	1988 ± 2		1989
7	11.33	2.90	2.71	1987 ± 2	1987 ± 2	1988	1987
8	13.15	3.37	3.13	1985 ± 2	1985 ± 2		1986
9	14.97	3.79	3.58	1984 ± 2	1983 ± 2		1984
10	16.62	4.12	3.95	1982 ± 2	1982 ± 1	1982	1983
11	18.33	4.55	4.34	1980 ± 2	1980 ± 2		1981
12	20.49	5.11	4.83	1978 ± 2	1978 ± 2	1979	1979
13	22.97	5.75	5.43	1976 ± 2	1976 ± 3		1977
14	25.38	6.27	6.01	1974 ± 2	1973 ± 2	1975	1975
15	27.70	6.84	6.56	1972 ± 2	1971 ± 2		1973
16	30.01	7.36	7.10	1969 ± 2	1969 ± 2	1971	1971
17	32.25	7.82	7.59	1967 ± 2	1967 ± 2		1969
18	34.50	8.35	8.09	1965 ± 2	1965 ± 2	1967	1967
19	36.71	8.85	8.60	1963 ± 2	1963 ± 2		1965
20	39.03	9.45	9.15	1961 ± 2	1961 ± 3	1962	1963
21	41.50	10.03	9.74	1959 ± 2	1958 ± 2		1960
22	43.87	10.53	10.28	1956 ± 2	1956 ± 2	1957	1958
23	46.32	11.13	10.83	1954 ± 3	1954 ± 2		1956
24	48.95	11.77	11.45	1951 ± 3	1951 ± 3	1953	1953
25	51.53	12.39	12.08	1949 ± 2	1949 ± 3		1950
26	54.12	12.98	12.68	1947 ± 3	1946 ± 2	1948	1947
27	56.74	13.60	13.29	1944 ± 3	1944 ± 3		1944
28	59.17	14.07	13.84	1942 ± 2	1941 ± 2	1942	1941
29	61.55	14.67	14.37	1939 ± 2	1939 ± 3		1939
30	63.99	15.20	14.93	1937 ± 2	1937 ± 2	1935	1936
31	66.39	15.75	15.48	1935 ± 2	1935 ± 2		
32	68.87	16.41	16.08	1933 ± 2	1932 ± 3		
33	71.30	16.93	16.67	1930 ± 2	1930 ± 2		
34	73.56	17.42	17.17	1928 ± 2	1928 ± 2		
35	75.78	17.94	17.68	1926 ± 2	1926 ± 2		
36	78.06	18.48	18.21	1924 ± 2	1924 ± 2		
37	80.57	19.13	18.81	1921 ± 3	1921 ± 3		
38	83.24	19.65	19.39	1919 ± 3	1919 ± 2		
39	86.16	20.36	20.01	1916 ± 3	1916 ± 3		
40	90.15	22.22	21.29	1912 ± 5	1911 ± 8		

* Calculation based on a Multiple Linear Regression with an R^2 of 0.9991 and a Standard Error of 0.6764.

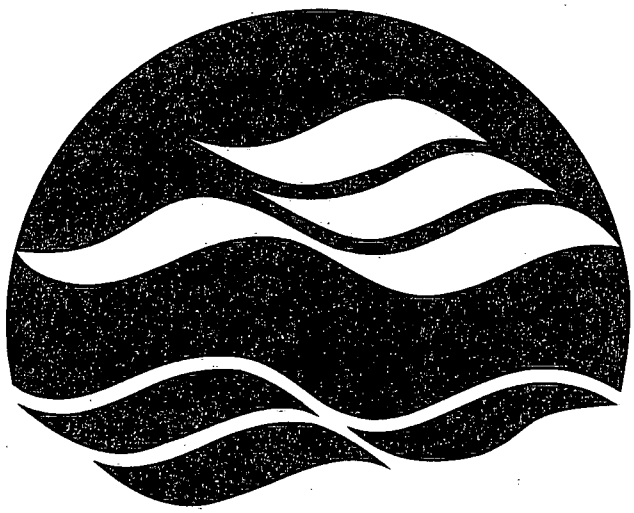

NATIONAL WATER RESEARCH INSTITUTE

INSTITUT NATIONAL DE RECHERCHE SUR LES EAUX

National Water Research Institute
Environment Canada
Canada Centre for Inland Waters
P.O. Box 5050
867 Lakeshore Road
Burlington, Ontario
Canada L7R 4A6

Institut national de recherche sur les eaux
Environnement Canada
Centre canadien des eaux intérieures
Case postale 5050
867, chemin Lakeshore
Burlington; (Ontario)
Canada L7R 4A6

National Hydrology Research Centre
11 Innovation Boulevard
Saskatoon, Saskatchewan
Canada S7N 3H5

Centre national de recherche en hydrologie
11, boulevard Innovation
Saskatoon; (Saskatchewan)
Canada S7N 3H5

Environment Canada Environnement Canada

Canada